Influence of Thermal History on Process–Properties Relationship in Fused Filament Fabrication of High-Temperature Thermoplastic Composites

Minh-Tam Nguyen[1], Cédric Courcoux[1], Daniel Therriault[1] and Martin Levesque[1*]

[1] Laboratory for Multiscale Mechanics (LM^2), Department of Mechanical Engineering, Polytechnique Montreal, Montreal, QC., H3T 1J4, Canada

**Martin Levesque (martin.levesque@polymtl.ca)*

Keywords: *Carbon fiber-reinforced Polyetherketoneketone; Fused filament fabrication; Mechanical performance, Thermal history*

1. Abstract

This study seeks a better understanding of the materials process-properties-structure relationship during the Fused Filament Fabrication (FFF) of short carbon fiber (CF)-reinforced high-temperature thermoplastics to improve the layer adhesion, thereby improving the mechanical performance of printed parts. A focus is placed on the unique thermal history of a printed part during printing, which is influenced by nozzle path and layer deposition time. The thermal history is characterized by the contact temperature between a depositing filament and the previously solidified adjacent material, or, interlayer adhesion temperature. Commercial short CF-reinforced polyetherketoneketone (PEKK-CF) filament is used to print structures with varying layer deposition times by varying the number of instances of the structure printed at once. Single edge-notch bending (SENB) specimens are cut from the printed walls to investigate the mechanical properties normal to the interface between printed layers. This method of specimen extraction eliminates the variation in thermal history that occurs when specimens of different geometries are printed individually. The mechanical properties results and structural observations show that with varying layer times, the interlayer adhesion temperature differs and affects the part's print quality and mechanical performance. Consequently, even with identical printing parameters such as nozzle temperature, bed temperature, chamber temperature, printing speed, and layer height, interlayer adhesion and mechanical properties can vary significantly between printed parts. These findings must be taken into account when interpreting mechanical performance, for determining the optimal slicing of complex geometries with varying layer times, and for scaling up the FFF manufacturing process to larger components.

2. Introduction

Successful additive manufacturing (AM) of thermoplastic composites requires understanding the relationship between the material, the printing process, and the resulting properties. Fused Filament Fabrication (FFF) is an extrusion-based AM process which heats a polymer or composite filament and deposits it layer by layer, allowing for the manufacturing of customized geometries in a single process, reducing waste and tooling costs [1]. High-temperature thermoplastics such as PEKK or the similar polyetheretherketone (PEEK) have superior thermal and mechanical properties in comparison to the commodity thermoplastics being commonly processed with FFF, with service temperatures of up to 140°C, or up to 250°C with carbon fiber reinforcement [2]. Adding short carbon-fiber reinforcement increases mechanical properties such as stiffness and strength, while decreasing thermal expansion and increasing thermal conductivity which improves geometric accuracy in the printed parts [1]. However, numerous challenges are encountered when printing high-temperature thermoplastics, both with and without carbon fiber reinforcement, due to their high processing temperatures and high thermal expansion, which lead to poor interlayer adhesion [2], [3]. Reported tensile strength values of FFF-printed PEEK average to 45% of their injection molded counterparts [4].

Since the mechanisms that drive interlayer adhesion, including molecular diffusion, entanglement and crystallization, are temperature dependent, it follows that the thermal history of the part during FFF would affect the interfacial strength between deposited filaments [4]. Few studies have investigated FFF of PEKK-CF, when compared with other high-temperature thermoplastic composites, such as polyetherimide-CF (PEI-CF) and polyetheretherketone-CF (PEEK-CF). Moreover, the limited existing studies in the literature do not address the effect of thermal history on the mechanical properties [2]. In our study, characterizing the interlayer fracture mechanics is of particular interest since it is the weakest build orientation in FFF-printed parts [5], [6]. We build upon previous work that has been done to link the effect of thermal history to interlayer adhesion in FFF for polylactide acid (PLA) [7], polypropylene (PP) [8], and neat PEKK [9], which discuss how interlayer time might affect interlayer bonding and thereby mechanical properties.

The objective of our study is to clarify the influence of interlayer adhesion temperature history on the interlayer fracture mechanics of FFF-printed PEKK-CF parts. This understanding will be critical when aiming to scale up the FFF process, since larger part geometries will result in higher layer deposition times.

3. Methodology

3.1. Materials

The commercially-available short carbon fiber reinforced polyetherketoneketone (PEKK-A-CF) filament used in this study was supplied by Nanovia (France). The filament was dried in a vacuum oven at 110°C for at least 12 hours prior to printing.

3.2. *Specimen fabrication*

The Hylo™ (AON3D, Canada), an FFF 3D printer equipped with a closed heated chamber and a heated bed, was used to print the walls (i.e. a vertical plate with a base to maintain equilibrium while printing) from which all the specimens were cut (see Figure 1). PrusaSlicer 2.9.4 software (Prusa Research, Czech Republic) was used to slice the 3D models and set the printing parameters. The geometry of the printed wall was designed to allow for machining of a full set of test specimens from one wall. Two cases were defined, differing only in the number of wall copies printed simultaneously, layer by layer: either one or three. A schematic of the three-copy case can be seen in Figure 2. By changing the number of copies printed, we are changing the layer time from 13 seconds (1 copy) to 46 seconds (3 copies), and therefore the amount of time during which a section of deposited material cools before more material is deposited on top.

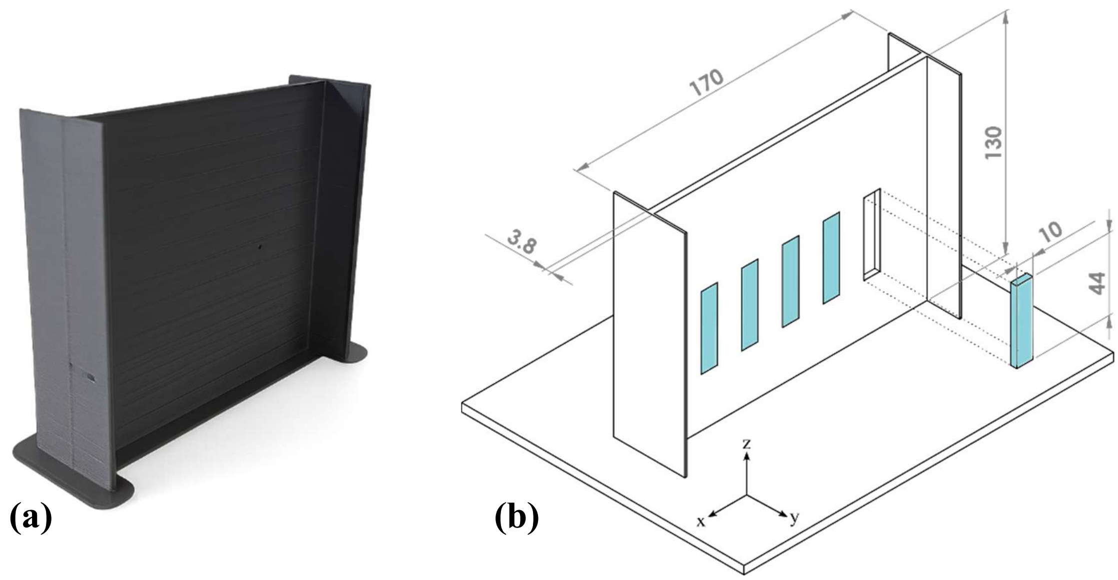

Figure 1. (a) photograph of one wall as printed, and (b) schematic of how the SENB specimens were machined from each wall, with placement and dimensions in millimetres.

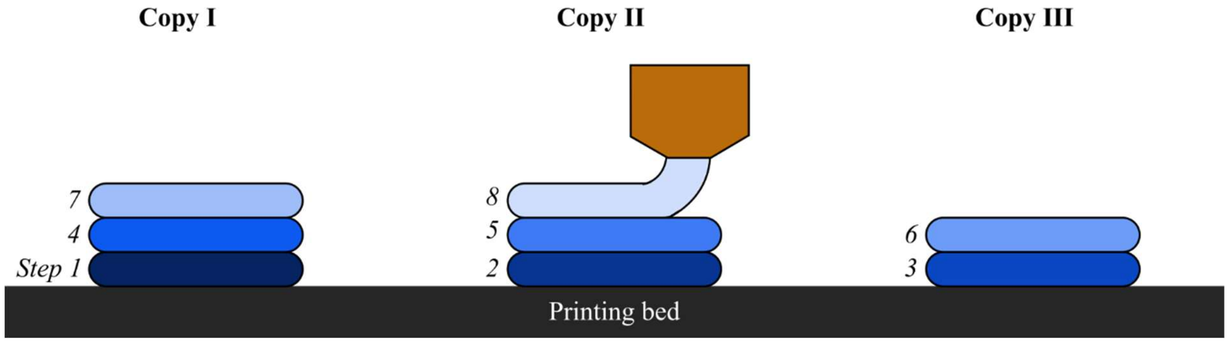

Figure 2. Schematic of the second case, where three copies of the same wall is printed at once, 'layer by layer' instead of 'object by object'. Sections of deposited material are labelled in the order of deposition: Step 1, 2, 3, etc. The bottommost layer for all three copies is printed first, then the next layer.

The most relevant printing parameters are listed in Table 1. These parameters were kept constant across the printing of different cases.

Table 1. Printing parameters used for all prints

Printing parameter	Value
Nozzle temperature [°C]	370
Bed temperature [°C]	150
Chamber temperature [°C]	150
Nozzle diameter [mm]	0.6
Nozzle speed [mm/s]	100
Layer height [mm]	0.4
Infill pattern	Aligned Rectilinear

Single-edge-notch bending (SENB) test specimens were machined from each wall, oriented such that the length of each specimen is aligned with the axis perpendicular to the plane of the printing bed, shown in Figure 1. Beams of 44 mm × 10 mm were cut using waterjet cutting (FLOW Mach 3, Flow, USA) from the wall. The notches were cut using a Buehler IsoMet Low Speed precision saw (Buehler, USA) with a blade 0.3 mm in thickness. Pre-cracks were created using a custom pendulum tapping set-up using a razor blade 0.2 mm thick.

The resulting notch with pre-crack was imaged and measured on both faces of each specimen using an Olympus SZX12 Stereo Microscope (Olympus Inc, USA) and a C-HP4 microscope camera (OPTIKA, Italy). The average total notch length for each specimen was compared to its width as measured using calipers to verify its compliance with the ASTM D5045 standard in maintaining a ratio between 0.45 and 0.55, and used later to compute K_{Ic}.

3.3. SENB testing

Flexural testing of the SENB specimens was performed in accordance with the ASTM D5045 standard on an MTS Insight electromechanical testing machine (MTS, USA) using a 1 kN load cell and 3-point-bend fixtures with a span length of 40 mm and a test rate of 1 mm/min.

Samples were then re-imaged post-testing to examine the crack propagation type that occurred.

3.4. Thermal model

A finite difference model with voxel activation developed by Courcoux et al. [10] was used to simulate the temperature of each point in the print throughout the deposition process. We account for natural convection and conduction through the bed and previously-deposited material, and assume a constant material density and thermal conductivity without the effect of temperature (T).

Table 2 presents the material parameters used to model our system, which were approximated from manufacturer data and measurements of similar materials. Figure 3 illustrates the thermal boundary conditions used, based on the printing parameters.

Table 2: Parameters used in the model for printing PEKK-CF in our system.

ρ $(\mathrm{kg.m^{-3}})$	c_p $(\mathrm{J.Kg^{-1}.K^{-1}})$	ε	$k_{filament}$ $(\mathrm{W.m^{-1}.K^{-1}})$	k_{bed} $(\mathrm{W.m^{-1}.K^{-1}})$	h_{air} $(\mathrm{W.m^{-2}.K^{-1}})$
1270	$(T - 100) * 3 + 1000$	0.9	0.4	0.9	5

We define interlayer adhesion temperature as the temperature of the voxel directly below the one being deposited (see Figure 3). By taking the average of this interlayer adhesion temperature across one deposited layer, we have a value to use to quantify the thermal history of a printed part. For the case where three copies of the wall were printed, layer by layer, for each given wall there is a period of time in between when each layer is deposited. This time is defined as a ‘cooling time’ within the model, where we assume there is no heating of the already printed wall from the nozzle.

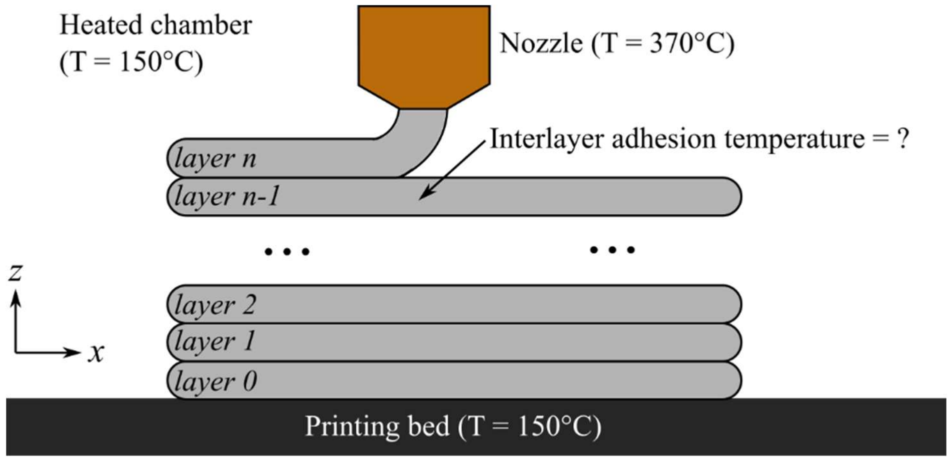

Figure 3. Schematic of temperature parameters and what we have defined as 'interlayer adhesion temperature' at a given point during the material deposition process.

This way, we can generate a different representative interlayer adhesion temperature value for each of the two cases: layer time of 13 seconds (1 copy), where the cooling time is 0; and layer time of 46 seconds (3 copies), where the cooling time is the difference (33 seconds).

The model has not been experimentally validated, but was used to indicate trends and compare the influence of cooling time, rather than to capture a validated representation of accurate exact temperatures for the two cases.

4. Results and Discussion

4.1. Thermal simulation

Figure 4(a) presents a 2D heat map of the simulated interlayer adhesion temperatures for a layer deposition time of 13 seconds. Varying values across the thickness of the wall (y-direction) have been averaged for simplicity. There is a temperature gradient for the layers printed close to the bed, but then a plateau is reached at about 233°C. Across the width of the section from which the SENB specimens were machined, there is no variation in temperature. The simulation results for a layer time of 46 seconds follow the same trends, but the plateau occurs at 186°C.

A more detailed view of the temperature profiles for the bottom 2.4 centimetres of both cases is shown in Figure 4(b). All the SENB specimens were cut above this section of the walls to avoid any influence of temperature variation on the mechanical results. While both cases plateau at a temperature above the glass transition temperature (T_g) of the filament material, the plateau simulated average interlayer adhesion temperature for the case where layer time is 13 seconds is significantly higher than for the case with layer time of 46 seconds.

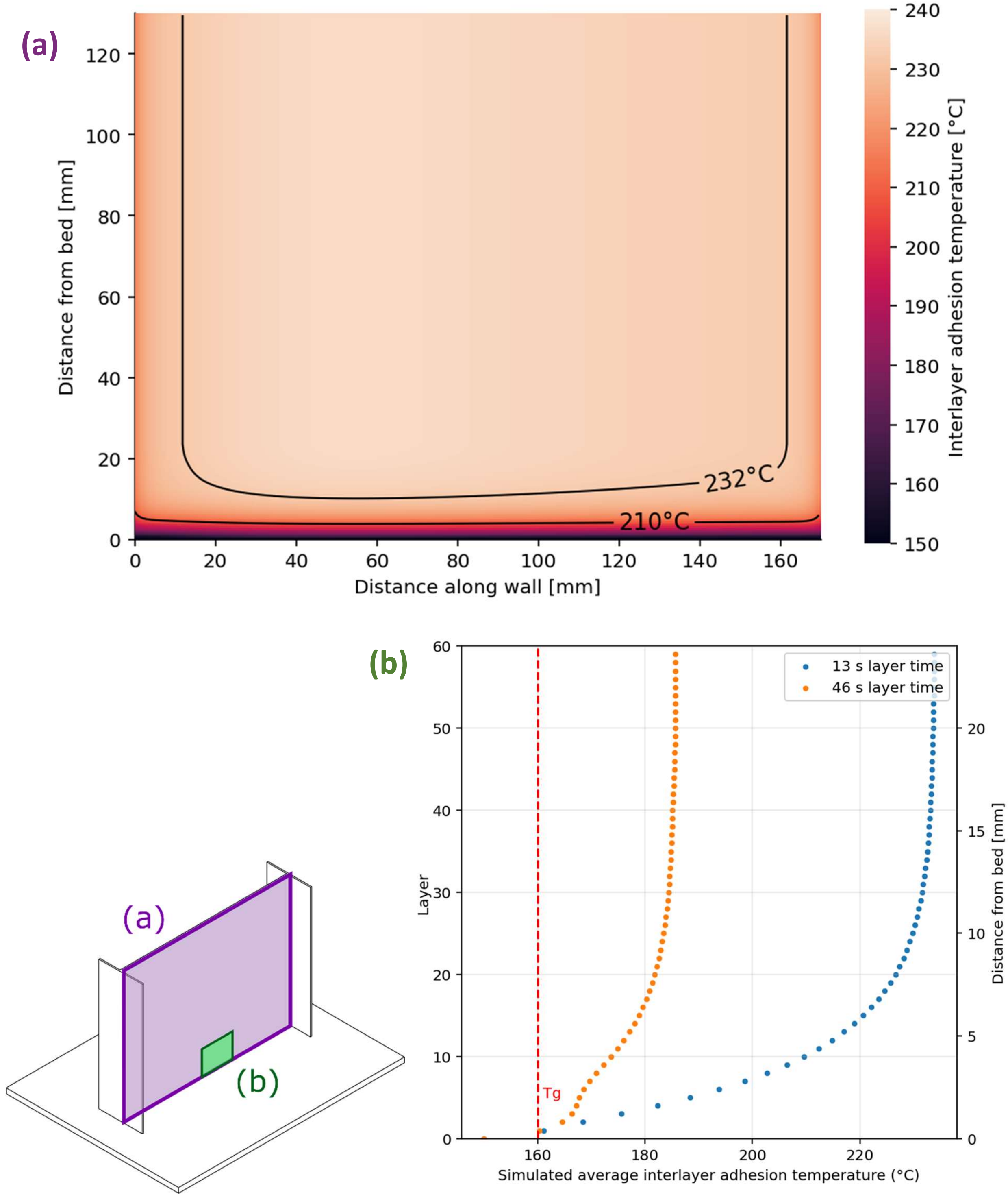

Figure 4. (a) 2D heat map of the interlayer adhesion temperature simulation results for the XZ plane of the wall printed with a layer time of 13 seconds. (b) Comparison of the average interlayer adhesion temperature results for both cases studied, for the first 60 layers printed.

4.2. Mechanical behaviour

Figure 5 shows the raw load-displacement curves from SENB testing for both cases, not normalized for cross-sectional area or crack length. The specimens cut from the wall printed with a layer time of 13 seconds exhibit brittle initial crack propagation, while the specimens cut from the wall printed with a layer time of 46 seconds exhibit ductile fracture behaviour. This observation was supported by post-mortem optical microscopy of the specimens, shown in Figure 6. The specimens printed with a 13 s layer time show a clean separation between the layers (Figure 6(a)) while the specimens printed with a 46 s layer time show plastic deformation and tearing at the interlayer adhesion zone (Figure 6(b)).

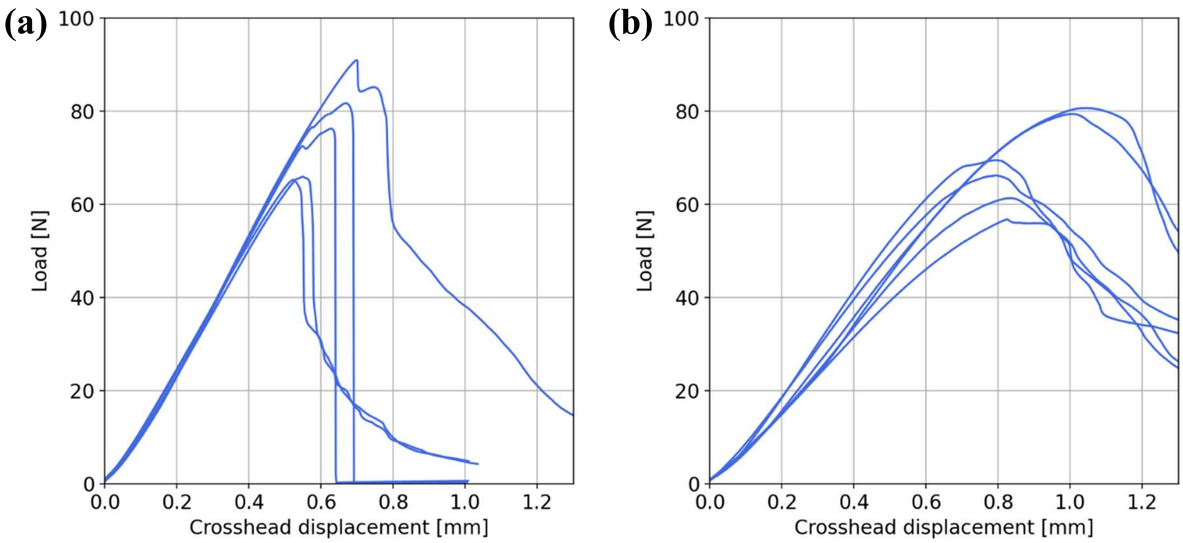

Figure 5. Load-displacement data for every specimen tested, cut from the walls (a) with layer time of 13 seconds (interlayer adhesion temperature of 233°C), and (b) layer time of 46 seconds (interlayer adhesion temperature of 186°C).

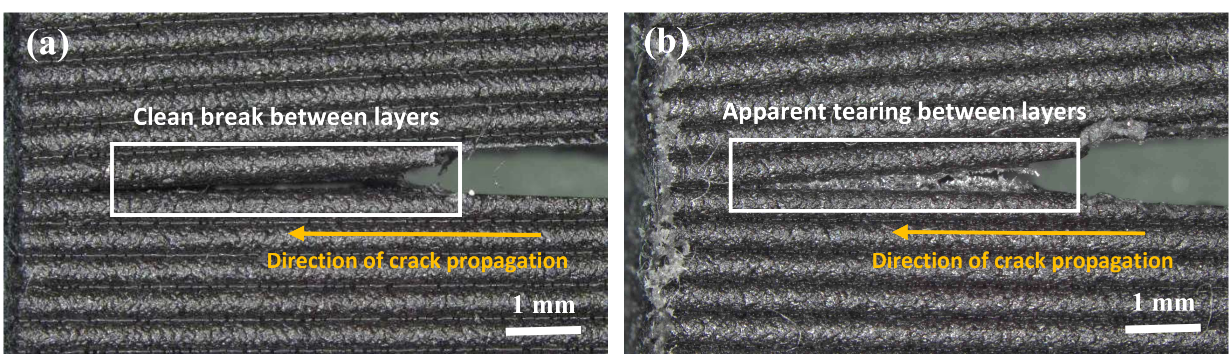

Figure 6. Optical microscopy of fracture cracks post-mortem for representative specimens cut from walls printed with a layer time of (a) 13 seconds (233°C) and (b) 46 seconds (186°C).

Figure 7 presents the computed K_{Ic} properties for both cases, and shows that the parts printed with a shorter interlayer time exhibit higher fracture toughness. With the computed 95% confidence intervals, we can conclude that the interlayer adhesion temperature has a statistically significant impact on K_{Ic}.

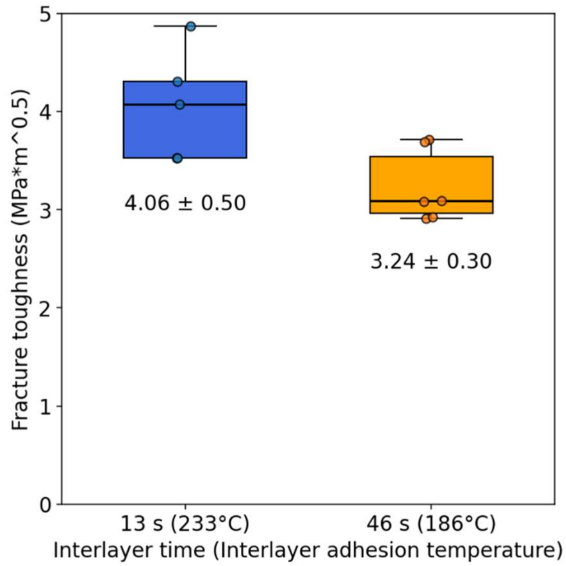

Figure 7. Box plot and individual data points of fracture toughness (KIc), calculated using each specimen's measured cross-sectional area and notch length. The mean and 95% confidence intervals are reported.

5. Conclusion

In this study, we defined interlayer adhesion temperature as a value to quantify thermal history, and used a numerical model to predict this value for two cases. The simulated plateau interlayer adhesion temperature for these two cases were spatially constant at 186°C and 233°C. Walls of the two cases were printed without varying any thermal printing parameters or nozzle speed. SENB testing of specimens machined from the two cases revealed a statistically significant difference in the computed K_{Ic} as function of interlayer adhesion temperature. The results suggest that the fracture toughness value of K_{Ic} increases when the interlayer adhesion temperature is increased. Thus, we have showed that FFF-printed parts with different thermal histories can display contrasting fracture behaviour, independent of printing parameters such as nozzle temperature, bed temperature, or chamber temperature.

Future work would be to further characterize the physical and mechanical differences in a range of cases. This methodology can also be used to study other materials used in extrusion-based AM. Improved understanding of the effect of interlayer adhesion temperature on mechanical properties can be used to inform more complex thermomechanical models for use in predictive simulations and for selection of processing parameters based on the geometry and size of a part. This will be critical to the development of higher productivity AM as a manufacturing process.

6. Acknowledgements

We are grateful to Dr. Dogan Arslan for his assistance with the selection of printing parameters for PEKK-CF. We acknowledge the financial and technical support of Safran Group and Dyze Design, and the financial support of NSERC (ALLRP 581752 - 23) and Prima Québec (R25 competition).

References

[1] M. Ahmadifar, K. Benfriha, M. Shirinbayan, and A. Tcharkhtchi, “Additive Manufacturing of Polymer-Based Composites Using Fused Filament Fabrication (FFF): a Review,” *Appl. Compos. Mater.*, vol. 28, no. 5, pp. 1335–1380, Oct. 2021, doi: 10.1007/s10443-021-09933-8.

[2] T. Yap, N. Heathman, T. Phillips, J. Beaman, and M. Tehrani, “Additive Manufacturing of Polyaryletherketone (PAEK) polymers and their composites,” *Compos. Part B Eng.*, vol. 266, p. 111019, Nov. 2023, doi: 10.1016/j.compositesb.2023.111019.

[3] P. K. Penumakala, J. Santo, and A. Thomas, “A critical review on the fused deposition modeling of thermoplastic polymer composites,” *Compos. PART B-Eng.*, vol. 201, p. 108336, Nov. 2020, doi: 10.1016/j.compositesb.2020.108336.

[4] J. Pu, C. McIlroy, A. Jones, and I. Ashcroft, “Understanding mechanical properties in fused filament fabrication of polyether ether ketone,” *Addit. Manuf.*, vol. 37, p. 101673, Jan. 2021, doi: 10.1016/j.addma.2020.101673.

[5] Z. Zhang, D. Yavas, Q. Liu, and D. Wu, “Effect of build orientation and raster pattern on the fracture behavior of carbon fiber reinforced polymer composites fabricated by additive manufacturing,” *Addit. Manuf.*, vol. 47, p. 102204, Nov. 2021, doi: 10.1016/j.addma.2021.102204.

[6] A. Lingua, N. Piccirelli, D. Therriault, and M. Lévesque, “In-situ full-field measurements for 3D printed polymers during mode I interface failure,” *Eng. Fract. Mech.*, vol. 269, p. 108483, Jun. 2022, doi: 10.1016/j.engfracmech.2022.108483.

[7] F. Lambiase, F. Pace, E. Andreucci, and A. Paoletti, “The effect of the interlayer time and deposition speed on the tensile properties of material extrusion components,” *Int. J. Adv. Manuf. Technol.*, vol. 133, no. 11, pp. 6111–6121, Aug. 2024, doi: 10.1007/s00170-024-14111-8.

[8] Y. Xu, M. Huang, and A. K. Schlarb, “Print path-dependent contact temperature dependency for 3D printing using fused filament fabrication,” *J. Appl. Polym. Sci.*, vol. 139, no. 24, p. 52337, 2022, doi: 10.1002/app.52337.

[9] A. Lepoivre, N. Boyard, A. Levy, and V. Sobotka, “Methodology to assess interlayer quality in the material extrusion process: A temperature and adhesion prediction on a high performance polymer,” *Addit. Manuf.*, vol. 60, p. 103167, Dec. 2022, doi: 10.1016/j.addma.2022.103167.

[10] C. Courcoux, D. Therriault, and F. Gosselin, “In-Situ monitoring of 3D printing process for Data Fusion using Kalman Filter,” *CANCOM*, Vancouver, Canada, 2026